Acta Oceanol. Sin., 2017, Vol. 36, No. 8, P. 20–33
DOI: 10.1007/s13131-017-1027-x
http://www.hyxb.org.cn
E-mail: hyxbe@263.net

Slowdown of sea surface height rises in the Nordic seas and related mechanisms

SHI Wenqi[1, 2]*, ZHAO Jinping[1], LIAN Xihu[3], WANG Xiaoyu[1], CHEN Weibin[2]

[1] School of Marine Environment, Ocean University of China, Qingdao 266100, China

[2] National Marine Environmental Monitoring Center, Dalian 116023, China

[3] Numerical Simulation Laboratory, North China Sea Marine Forecasting Center, Qingdao 11600, China

Received 31 March 2016; accepted 23 August 2016

Abstract

A slowdown of sea surface height (SSH) rise occurred in the Nordic (GIN) seas around 2004. In this study, SSH satellite data and constructed steric height data for the decades before and after 2004 (i.e., May 1994 to April 2014) were used for comparative analysis. The findings indicate that the rate of slowdown of SSH rises in the GIN seas (3.0 mm/a) far exceeded that of the global mean (0.6 mm/a). In particular, the mean steric height of the GIN seas increased at a rate of 4.5 mm/a and then decreased at a slower pace. This was the main factor responsible for the stagnation of the SSH rises, while the mass factor only increased slightly. The Norwegian Sea particularly experienced the most prominent slowdown in SSH rises, mainly due to decreased warming of the 0–600 m layer. The controlling factors of this decreased warming were cessation in the increase of volume of the Atlantic inflow and stagnation of warming of the inflow. However, variations in air-sea thermal flux were not a major factor. In the recent two decades, mean halosteric components of the GIN seas decreased steadily and remained at a rate of 2 mm/a or more because of increased flow and salinity of the Atlantic inflow during the first decade, and reduction in freshwater inputs from the Arctic Ocean in the second decade.

Key words: Nordic seas, sea surface height, steric height, slowdown in sea level rises

Citation: Shi Wenqi, Zhao Jinping, Lian Xihu, Wang Xiaoyu, Chen Weibin. 2017. Slowdown of sea surface height rises in the Nordic seas and related mechanisms. Acta Oceanologica Sinica, 36(8): 20–33, doi: 10.1007/s13131-017-1027-x

1 Introduction

Sea level change, an important phenomenon of climate change (CC), is sensitive to climatic processes and has significant regional differences (IPCC, 2013). Owing to factors such as warming of seawater and melting of glaciers as a result of CC, the global mean sea level has been in a state of steady increase (Cazenave et al., 2014). However, the rate of rise declined significantly around 2004 (Ablain et al., 2009). The decline was generally considered as having been caused by ENSO-related natural variations. A major El Niño event occurred in 1997/1998. After that, La Niña was the predominant phase over the past decade, during which surface cooling occurred in the Pacific Ocean and terrestrial precipitation increased. These two factors resulted in stagnation of sea level rises. Nevertheless, the global mean sea level had risen steadily after the ENSO effect was eliminated (Cazenave et al., 2012, 2014).

The Nordic seas—the Greenland, Iceland, and Norwegian (GIN) seas—have very unique sea territories. Being a relatively closed system, sea level changes in GIN seas show obvious regional characteristics. With the Greenland ice sheet undergoing drastic melting in the recent period (IPCC, 2013), a part of its meltwater would have entered the GIN seas, affecting the characteristics of sea level changes in this region. At the same time, the GIN seas collectively act as a channel connecting the Arctic and Atlantic Oceans (Fig. 1). As the Arctic Ocean is rapidly changing, it inevitably affects sea level changes in the GIN seas. Studies have found a trend of significant slowdown of sea level rises in the GIN seas in the recent decades (Jiang et al., 2011). Hence, in-depth studies on the changing processes of levels of the GIN seas and their relationship with the North Atlantic meridional overturning circulation and CC would be of great significance.

There are two factors mainly responsible for changes in non-tidal absolute sea levels: steric changes and mass changes of water columns. Steric changes refer to variations in the thermohaline properties of seawater caused by air-sea buoyancy flux and oceanic thermohaline advections, as well as the resultant density changes. These changes affect the steric height of water columns and are collectively known as the steric effect, which comprises thermosteric and halosteric components. It is generally believed that the global steric height is mainly influenced by the thermosteric effect (Mork and Skagseth, 2005; Siegismund et al., 2007). However, the halosteric effect may be dominant in certain sea territories (Antonov et al., 2002; Ivchenko et al., 2007).

Mass changes of water columns mainly arise from variations in total seawater volume caused by melting glaciers, which in turn affect the height of water columns. Other causes of mass changes include redistribution of marine columns due to wind field variations and water exchanges between the ocean and atmosphere/land (Cazenave et al., 2014).

There have been many studies on changes in the sea surface height (SSH) of the GIN seas. Mork and Skagseth (2005) analyzed seasonal variations in the SSH of the GIN seas and found that the

Foundation item: The National Natural Science Foundation of China under contract No. 41330960; the National Major Scientific Research Program on Global Changes under contract No. 2015CB953900.
*Corresponding author, E-mail: swqouc@163.com

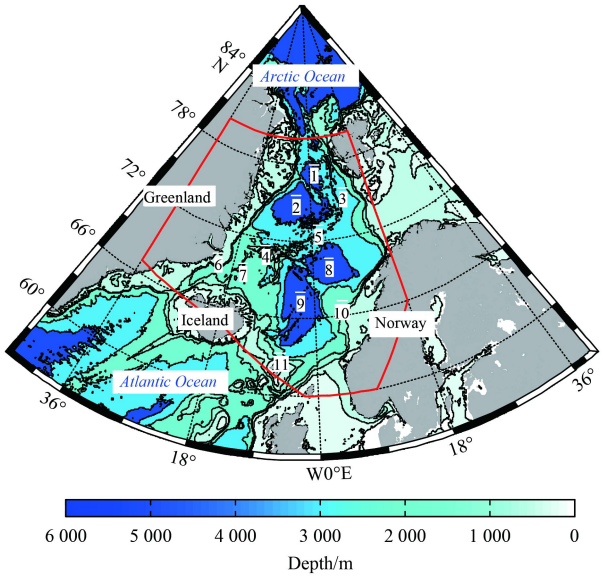

Fig. 1. Topographic map of the GIN seas and surrounding waters. Blue shades represent depth (m) and the sea territory enclosed by the red frame is the extent of the GIN seas selected for this study. The geographical locations represented by the various numbers are as follows: 1. Boreas Basin, 2. Greenland Basin, 3. Knipovich Ridge, 4. Jan Mayen Fracture Zone, 5. Mohn Ridge, 6. Kolbeinsey Ridge, 7. Icelandic Plateau, 8. Lofoten Basin, 9. Norwegian Basin, 10. Vøring Plateau, and 11. Faroe Islands.

steric effect accounted for only 40% of changes in SSH, whereas the mass component was mainly responsible. For this sea territory, the steric effect was mainly the result of net thermal flux in the upper water. Siegismund et al. (2007) used a relatively complete set of thermohaline data to study the characteristics of changes in the steric height of the GIN seas at multiple temporal scales and concluded that they predominantly experienced seasonal variations. Contributions of the thermosteric component to steric height represented a north-south dipole, which significantly affected steric height variabilities in the eastern sea territories. Henry et al. (2012) calculated and analyzed the ratios of steric height and the mass component contributing to fluctuations in water level at tidal stations along the Norwegian coast and found that the proportion of the latter began to increase from 2003.

Mork et al. (2014) analyzed the thermal and freshwater contents in the upper water of the Norwegian Sea (σ_t=27.9 and above) between 1951 and 2010 and found significant interdecadal characteristics for changes in both types of contents; positive anomalies for both occurred in the 1960s and 2000s, while negative anomalies occurred during the late 1960s and early 1990s. The larger the amount of both contents, the greater was the corresponding steric height, indicating the existence of interdecadal differences in steric height of the GIN seas. Shao and Zhao (2015) found uneven correlational spatial distributions between the anomalies of the SSH and steric height of the GIN seas. The correlation between both indicators at the Lofoten and northern Norwegian Basins was strong, but that between the anomalies of SSH and steric height were weakest at the northeastern Norwegian Sea. The annual amplitudes of the average SSH and steric height anomalies for the GIN seas region were basically similar between 1996 and 2002. However, the amplitude of the latter comprised less than 50% of the former after 2006.

To date, direct researches have not yet been conducted on the slowdown in sea level rises of the GIN seas, which occurred only in recent years. In this study, we first analyze the characteristics of the slowdown and compare it with global mean results. Next, we discuss the contributions of the steric effect and mass changes to the slowdown. Finally, the related mechanisms are analyzed and the underlying causes investigated.

2 Data and calculation methods

2.1 *Satellite data*

In this study, satellite data on sea level anomalies (SLA) were obtained from the DUACS 2014 multi-satellite integrated monthly average data provided by the Centre National d'Etudes Spatiales (CNES), the French government space agency (http://www.aviso.oceanobs.com/duacs/). This set of data uses the Mercator projection, has a horizontal resolution of (1/4)°×(1/4)°, and has been calibrated for atmospheric pressure, tidal movements, and the dry tropospheric effect. The DUACS 2014 SLA data were based on the mean sea level (MSS) for 1993–2012. As the height of the fixed terrestrial ellipsoid is used as reference for MSS, the SLA data contain signals on relative sea level changes caused by movements of the earth's crust over that period. In this case, these movements were mainly the effects of glacial isostatic adjustments (GIA).

Tamisiea and Mitrovica (2011) provided an impact distribution map of sea level changes by measuring the GIA effect with an altimeter (Fig. 3b in their paper). Their findings indicate that for the GIN seas, the impact of the GIA effect on sea level trends did not exceed 0.15 mm/a and thus, could be ignored.

Using actual measurements, Volkov and Pujol (2012) verified that AVISO's altimeter data were suitable for studying sea level changes and surface currents of the GIN seas. And a comparison of trends obtained from tide gauge records and SLA interpolated to the locations of tide gauges (from Table 4 of their paper) shows that trends agree in sign, the difference between them at GIN seas stations is less than 3 mm/a, and the average of the differences at 5 GIN seas stations is about 2.1 mm/a. So the error of trend from AVISO data should be about 2 mm/a.

The duration of the acquired satellite data was from 1993 to the end of 2014. In the SLA data, substantial areas of the GIN seas were not measured for January–March 1994. Hence, 20 years of SLA data from May 1994 until April 2014 were extracted for analysis. During this period, satellite altimeter data for some areas in the northeastern sea territories of Greenland were unmeasured. Thus, the spatial grids corresponding to these missing areas were excluded from the study. Existing research indicate that the slowdown in sea level rises of the GIN seas occurred around 2004 (Jiang et al., 2011). As such, the aforementioned set of data was divided into two subsets of one decade each: May 1994–April 2004 and May 2004–April 2014. Comparative analyses were then conducted on the differences in the rate of sea level rises between those two periods.

SLA changes comprise the sum of changes in steric height and the mass component. There are two types of observational data for the mass component: (1) single-point data measured by pressure sensors on the seabed and (2) gravity satellite data. The first type of data is scarcer and does not meet the spatial scale requirements for this study. Among the second type of data, GRACE gravity satellite data is widely used nowadays and are of good quality (Volkov and Landerer, 2013; Chambers and Bonin, 2012). However, available data only commenced from 2003, while battery replacement and maintenance around 2011 resulted in poorer data quality for a period of time. The GRACE data

also did not include measurements for substantial areas of the GIN seas, while deviations for the measured areas were large (approximately 7 mm). Thus, the duration and quality of this data made them unsuitable for our analysis.

Theoretically, the mass component could be obtained by subtracting steric height from SLA, but a problem arises in that the error for the resultant mass component will be large because it is the sum of errors for both SLA and steric height. Because data with sufficient duration and accuracy were not available, the mass component was not analyzed specifically in this study. Instead, the focus was on steric height changes. In the rest of this paper, we describe steric height as the main component contributing to the stagnation of SSH rises in the GIN seas.

2.2 *Hydrological and meteorological data*

In this study, the hydrological data used for calculating steric height were extracted from the average monthly reanalysis data from the EN4 hydrological dataset provided by Met Office, the United Kingdom (Good et al., 2013). The data were compiled from many observational data, which mainly included those from the World Ocean Database (WOD), Global Temperature and Salinity Profile Project (GTSPP), Argo, and Arctic Synoptic Basin-wide Observations (ASBO). Thus, degree of credibility is high. The horizontal resolution of the data is 1°×1°, and the area covered is 83°–89°N, 1°–360°E. There were 42 vertical layers, with thickness of the water layers ranging from 10 m at the surface to 300 m in the deep ocean.

The SLA data was interpolated to similar grid points of the hydrological data because their grids were not consistent. In the interpolation method, the average value for the 16 SLA grid points contained within each hydrological grid was obtained. If the SLA data for eight or more grid points within a hydrological grid were unmeasured, the average value for that area was also considered to be unmeasured.

The meteorological data used were the 12-hour forecast data from the ERA-interim reanalysis data provided by ECMWF (European Centre for Medium Range Weather Forecasts). The main parameters used included short- and long-wave radiations, latent and sensible thermal fluxes, rates of evaporation and precipitation, and wind fields (Dee et al., 2011).

2.3 *Calculation of steric height*

The formulas for calculating steric height provided in various literature are basically similar (Siegismund et al., 2007; Gill and Niller, 1973; Tabata et al., 1986). However, Siegismund et al. (2007) proposed calculation formulas tailored to the Cartesian coordinate system, including error analysis. As this method is more rational, it was used to calculate steric height in this study. The calculation formulas are as follows:

$$h'(t)=\frac{1}{g}\int_{P_{H_0}}^{P_0}h'(z,t)\mathrm{d}p\approx\int_{H_0}^{0}h'(z,t)\mathrm{d}z=\int_{H_0}^{0}\left(\frac{\rho_0}{\rho}-1\right)\mathrm{d}z, \quad (1)$$

$$\int_{H_0}^{0}h'^{\mathrm{T}}(z,t)\mathrm{d}z=\int_{H_0}^{0}\frac{\partial h'(T^*,S^*)}{\partial T}(T-T_0)\mathrm{d}z, \quad (2)$$

$$\int_{H_0}^{0}h'^{\mathrm{S}}(z,t)\mathrm{d}z=\int_{H_0}^{0}\frac{\partial h'(T^*,S^*)}{\partial S}(S-S_0)\mathrm{d}z, \quad (3)$$

$$l\frac{\partial h'}{\partial T}=-\frac{\rho_0}{\rho^2}\frac{\partial\rho}{\partial S}=\frac{\rho_0}{\rho}\alpha,$$

$$\frac{\partial h'}{\partial S}=-\frac{\rho_0}{\rho^2}\frac{\partial\rho}{\partial S}=-\frac{\rho_0}{\rho}\beta,$$

where h' is steric height (SH); h'^{T} is the proportion of sea level changes caused by the thermosteric effect, or the thermosteric component (TC); h'^{S} is the proportion of sea level changes caused by the halosteric effect, or the halosteric component (SC); α and β are the thermal expansion and saline contraction coefficients at (P_z, S^*, T^*), respectively; and P_z is pressure at the depth of location z.

For the rest of this paper, steric height is calculated using Eq. (1), while the thermosteric and halosteric components are calculated using Eqs (2) and (3), respectively. The values adopted for the relevant parameters in the formulas are similar to that by Siegismund et al. (2007). The sum of the calculated thermosteric and halosteric components is basically similar to the steric height, and the vertical integral of the latter arranged within 0–1 500 m of the water column. Thus, H_0=1 500 m was adopted (Siegismund et al., 2007; Shao and Zhao, 2015).

3 Slowdown in SSH rises in the GIN seas

Presently, many studies have noted the consistent phenomenon of slowdown in global mean SSH rises. Observing the rate of global mean SSH rises considering altimeter data, Cazenave et al. (2014) concluded that the rate for 2003–2011 (2.4 mm/a) had decreased significantly compared to that for 1994–2002 (3.5 mm/a). According to Ablain et al. (2009), the rate of global mean SSH rises for 1993–2008 was 3.11 mm/a, while that for 2005–2008 was only 1.08 mm/a. A slowdown in the global mean SSH rises also occurred around 2004.

Taking into account the earth's curvature, we wanted to avoid exaggeration of the high-latitude characteristics. Hence, the area weighted average method was used to calculate the regional mean value. After comparing the global mean SLA curves obtained using weighted versus direct averaging, not much difference was found between the two. Using weighted averaging, the rates of global mean SLA rises for 1994–2002 and 2003–2011 were 3.4 and 2.8 mm/a, respectively. These were consistent with the results of Cazenave et al. (2014).

The rates of global mean SLA rises derived in this study for 1993–2008 and 2005–2008 were 3.3 and 2.6 mm/a, respectively. The magnitude of slowdown in the rate of rises was weaker compared to the findings of Ablain et al. (2009). This discrepancy could be a result of the different data and processing methods employed. Ablain et al. (2009) used the Jason-1 and T/P satellite data and low-pass filtering process for 60 days; this study used multi-satellite integrated data without any filtering process. Nevertheless, the rate of SSH rises obtained in this study is consistent with the results of earlier studies.

3.1 *Slowdown in SLA rises of the GIN seas*

Linear fitting was separately carried out using the global and GIN seas SLA data for the two periods described in Section 2.1, and the results are shown in Fig. 2. On average, the rates of mean SSH rises at the global scale and for the GIN seas over the past two decades were similar at approximately 3.0 mm/a (95% confidence level; unless otherwise specified, this level is used for all linear fittings in this paper). The rate of mean SLA rises in the GIN seas for the first decade was faster than the global mean;

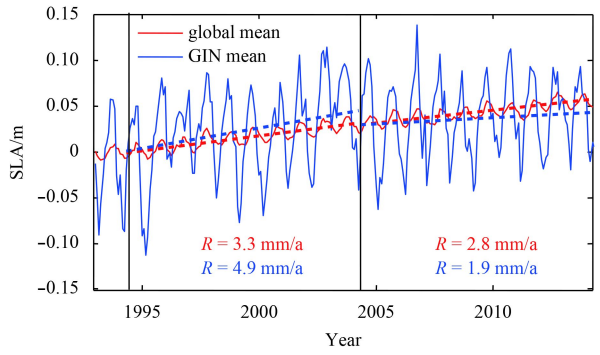

Fig. 2. Segmented linear fitting results for the trends of the global and GIN seas' mean SLA. Solid lines are trends based on actual measurements, while broken lines are results of linear fitting. *R* is the respective rate of change obtained from segmented linear fitting of the corresponding colored trends for the two periods.

however, the situation was completely reversed for the second decade. The magnitude of slowdown in SSH rises of the GIN seas was far greater than the global mean; the rate declined from 4.9 to 1.9 mm/a between the first and second decades. This represents a reduction of 3.0 mm/a, compared to the global reduction rate of 0.6 mm/a. It is obvious that the slowdown in SSH rises of the GIN seas is more prominent compared to other regions in the world.

The spatial distribution diagram (Fig. 3a) shows that the SLA for most of the regions in the GIN seas increased rapidly and significantly during 1994–2004. This was especially the case for the Lofoten Basin, where the rate of rise was 8 mm/a or more. However, there was no rapid increase in any region within the GIN seas during 2004–2014. Although the trend was slightly greater for the region around the Greenland Sea, it remained at 4 mm/a or below. Generally, there was no significant linear trend for most of the regions within the GIN seas (Fig. 3b).

Although stagnation of SSH rises occurred throughout most of the GIN seas, there were substantial spatial variations in terms of the magnitude of slowdown for SLA rises. There was a significant decrease in SLA rises at the Lofoten and Norwegian Basins (8 mm/a), while that for the Iceland Sea and along the Norwegian coast was approximately 4 mm/a. Overall, SLA rises remained unchanged at regions above 72°N, with only slight increases for some areas.

A comparison between Figs 3a and b reveals regions within the GIN seas that experienced larger rates of SSH rises for 1994–2004. The slowdown was also more prominent for these regions. Statistical computations showed that the Norwegian Sea region accounted for 80% of the slowdown in the GIN seas' mean SLA rises, with the Norwegian and Lofoten Basins (areas shaded red in Fig. 3c) having the most prominent slowdown rates. Although the combined areas of the two basins comprise only approximately 26% of the total area of the GIN seas, they accounted for approximately 50% of the total slowdown in the GIN seas' mean SLA rises. Thus, these two basins were the main regions contributing towards the stagnation in mean SSH rises of the GIN seas.

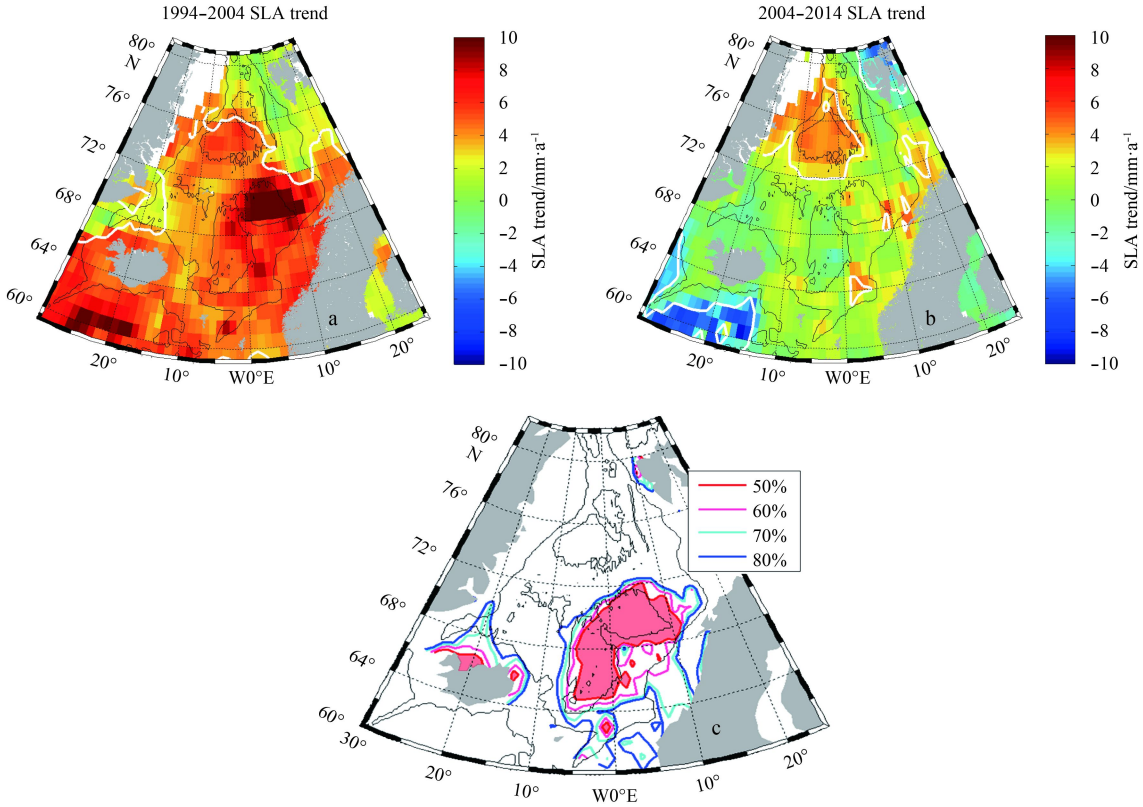

Fig. 3. Trends of SLA in the GIN seas. a. Spatial distribution for 1994–2004, b. spatial distribution for 2004–2014, and c. cumulative contribution of extreme values to magnitude of slowdown in SLA rises. SLA trends were obtained through direct linear fitting of monthly mean data. The black lines in this and subsequent spatial distribution figures represent 1 000 and 3 000 m bathymetrical contour lines. Regions for which linear fitting results passed the 95% confidence level are encompassed by white lines.

3.2 *Changes in steric height*

The EN4 hydrological data were derived by assimilating collected and actual measured data of thermohaline profiles. As adequate sectional observational data of the GIN seas after 1980 (Siegismund et al., 2007) are available, EN4 assimilated data for that region post-1980 are deemed to be highly credible. Therefore, data since 1980 were considered in the construction of steric height in this study, accounting for 35 years of steric height fields for the GIN seas.

Between 1980 and 1995, the mean steric height for the GIN seas gradually increased and then rapidly decreased. Nevertheless, the overall trend for the entire period was still upwards. It then rose steadily at a rate of 2.5 mm/a during 1995–2004, followed by steady and significant decline at a rate of 2.0 mm/a during 2005–2014. The change in steric height rises was –4.5 mm/a, which was more than that for SLA rises (–3.0 mm/a). Thus, substantial declines in the rate of steric height changes were the main reason behind the stagnation of SLA rises in the GIN seas.

Steric height is essentially the sum of the thermosteric and halosteric components. The former increased steadily in 1981–1993, but declined rapidly in 1993–1998; the magnitude of change for both periods was similar. Subsequently, the thermosteric component increased rapidly, at a rate of 4.2 mm/a during 1995–2004. However, there was a slight downward trend after 2004 (Fig. 4b). The halosteric component behaved differently; it remained steady during 1980–1997 and only experienced minor fluctuations. This was followed by a significant and steady downward trend after 1997, at a rate of 2.0 mm/a (Fig. 4c). The difference of rates for the thermosteric component between during 2004–2014 and 1994–2004 was –4.6 mm/a, and that for halosteric component was –0.4 mm/a, respectively. Thus, the rapid rise and then rapid decline in steric height between 1994 and 2014 could be attributed to the stagnation in rise of the thermosteric component.

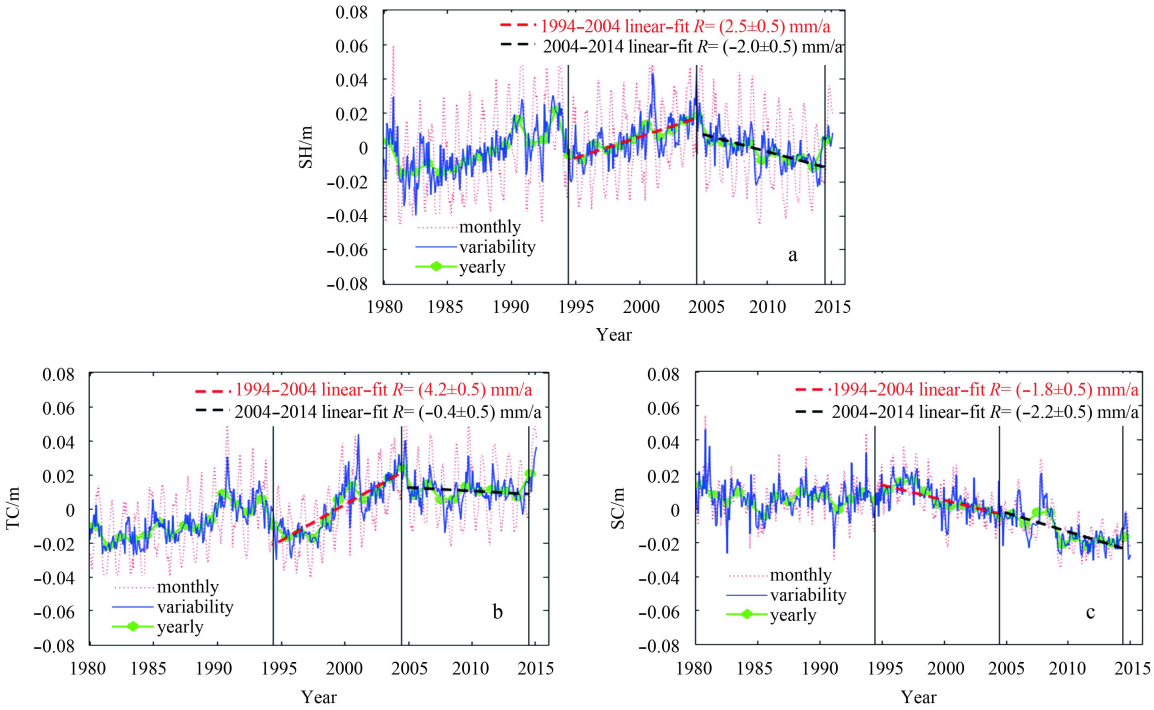

Fig. 4. Segmented fitting results for various trends of the GIN seas. a. Mean steric height (SH), b. thermosteric component (TC), and c. halosteric component (SC). The calculation range for the mean steric height of the GIN seas is similar to the area of coverage within the valid SLA data. The rate of change was obtained from anomaly data, i.e., segmented linear fitting of the blue lines.

From the results of the earlier analysis, it could be easily concluded that the recent stagnation of mean SLA rises in the GIN seas was largely the result of stagnation in rise of the thermosteric component, or in other words, stagnation in warming of the upper water. It is worth noting that the timing for stagnation of warming for the GIN seas coincided with that for the upper water of the Atlantic Ocean (please refer to Fig. 1b of Chen and Tung (2014); there was significant stagnation of warming for the upper water of the Atlantic Ocean around 2004).

The characteristic of steady salinization of the GIN seas around 1997 was a unique phenomenon post-1980. Past studies have shown that upper water of the GIN seas exhibited a general trend of desalination between the 1960s and 1990s (Siegismund et al., 2007; Blindheim and Østerhus, 2005; Furevik and Nilsen, 2005). The salinization of the upper water of the GIN seas in the recent two decades could either be a long-term development trend henceforth or the result of interdecadal fluctuations (or even fluctuations over a longer temporal scale). However, it can be confirmed only after continuous accumulation of data.

Changes in steric height are dependent on changes in the thermohaline properties of the upper water. The upper water of the GIN seas is directly affected by the Atlantic and Arctic inflows simultaneously, resulting in very complex internal circulations. There are large horizontal variations in the thermohaline properties of the water body in GIN seas, with different factors controlling the properties of the upper water in various sea territories (Rossby et al., 2009; Carton et al., 2011). Therefore, it is necessary to analyze the spatial characteristics of changes in steric height.

During 1994–2004, the steric height for most regions of the GIN seas rose rapidly and significantly. This was especially the case at the Lofoten Basin, where the rate was 8.0 mm/a or more (Fig. 5a). By 2004–2014, the steric height for most regions had de-

clined, with slow rises limited to a small portion of the sea territories (Fig. 5b). By comparing Figs 5a and b, significant slowdown in the rise of steric height can be observed for most regions of the GIN seas. For each period, the spatial distribution for rate of change for the thermosteric component of the GIN seas (Figs 5c and d) was consistent with that for the steric height (except for a small portion of sea territories along the eastern coast of Greenland). While, there were small temporal and spatial variations for the rate of change in the halosteric component, both of which were approximately –2.0 mm/a (Figs 5e and f).

Comparing the trends during 2004–2014 and 1994–2004, slowdown in rise of the halosteric component (–10.0 mm/a) was found only in a small portion of sea territories along the eastern coast of Greenland. The trend for most regions of the GIN seas remained unchanged. The aforementioned spatial distribution characteristic further confirmed that the thermosteric component was the major contributor to the substantial decline in rise of steric height in the GIN seas. The temporal variations and characteristic of spatial distribution of the steric height in GIN seas were found to be mainly affected by the thermosteric effect, which was consistent with the findings of previous studies (Mork and Skagseth, 2005; Siegismund et al., 2007). Unlike the findings of Shao and Zhao (2015), this study did not find a greater rate of decline in steric height along the Norwegian coast. This could be due to the different data for different durations used in the studies.

Two regions within the GIN seas experienced greater slowdown in steric height rises: the larger region is the sea territories around the Lofoten Basin, while the smaller region is off the northeastern coast of Greenland. Figure 5 shows that the former region was mainly affected by the thermosteric component, while slowdown in the latter was caused by the halosteric component. It should be noted that some sea territories off the northeastern coast of Greenland were unmeasured and missing from the SLA data. The area is also covered by sea ice throughout most of the year. Since further study is required to ascertain the applicability of Eqs (1)–(3) for calculating the steric height of ice-covered sea

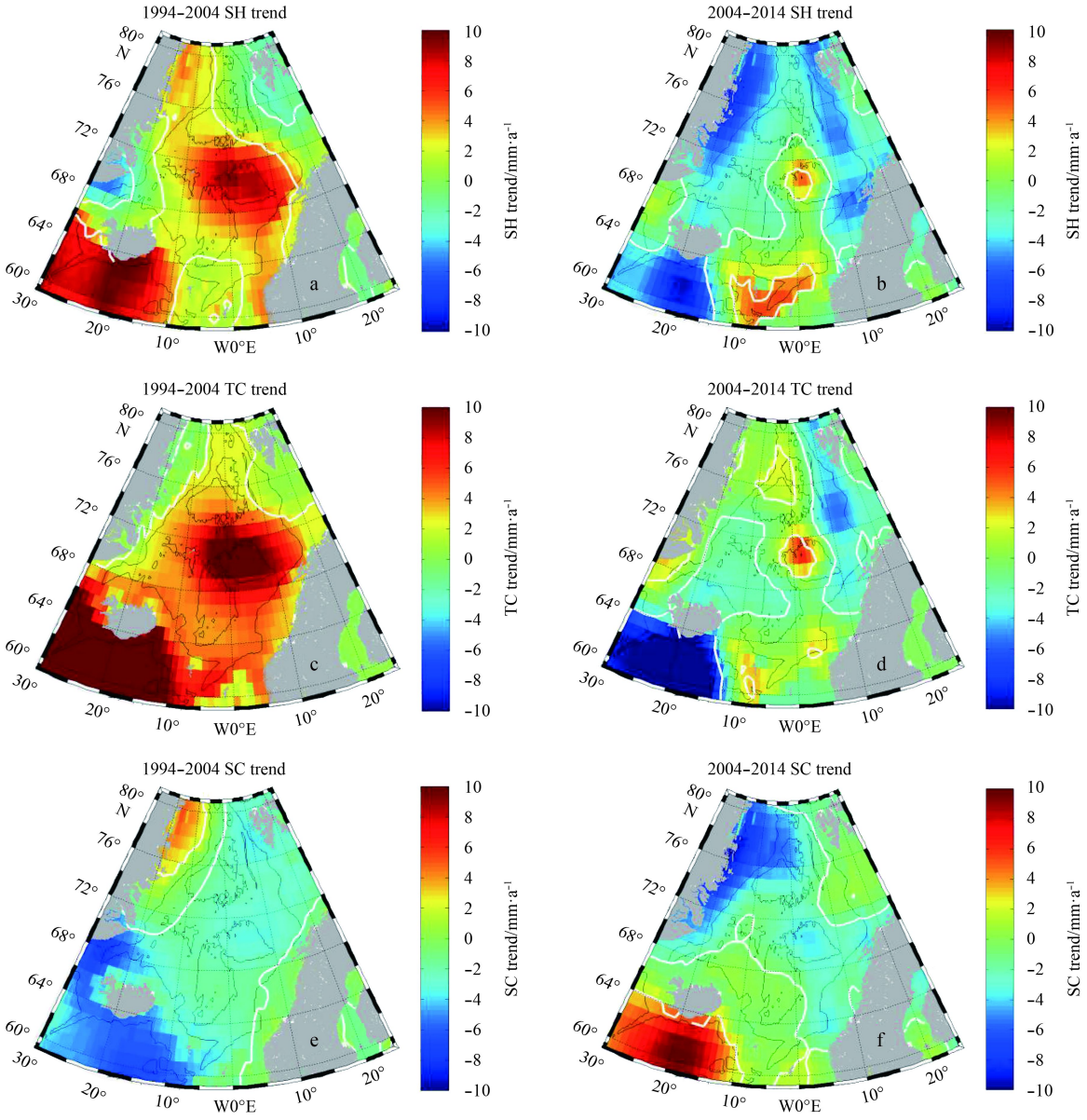

Fig. 5. Spatial distribution of trends of SH, TC and SC. Respective spatial distribution of mean SH (a, b), TC (c, d), and SC (e, f) trends for 1994–2004 and 2004–2014.

territories, changes in steric height for these sea territories are not discussed in this paper.

Within the GIN seas, the Lofoten and Norwegian Basins are more representative because slowdown in SSH rises and decrease in steric height rises were more prominent. Equation (1) shows that steric height is obtained from the $h'(z, t)$ integral for each layer. The mean trend of $h'(z, t)$ for each layer of the Norwegian Sea basins (Lofoten and Norwegian Basins) was calculated to determine changes in the characteristics of the steric height component for various layers. Applying the same principle, changes in the characteristics of the thermosteric and halosteric components were also processed.

Comparing the situation during 2004–2014 with that during 1994–2004 (Figs 6a and b), the main changes in trends of the steric height component ($h'(z, t)$, blue line in Fig. 6) were found to occur at the 0–600 m sea layer. The $h'(z, t)$ trend for this layer changed from positive in 1994–2004 to negative in 2004–2014, with a significant magnitude. For the thermosteric component ($h'^{T}(z, t)$), slowdown in the rise occurred within the 0–500 m layer (red line in Fig. 6), with the magnitude of slowdown increasing as it approaches the surface layer. This was consistent with the characteristic of vertical distribution for the $h'(z, t)$ trend. In sea layers deeper than 600 m, the variations for both $h'(z, t)$ and $h'^{T}(z, t)$ were small and did not show any significant change. Thus, the 0–600 m sea layer was the main layer responsible for the slowdown in steric height of the GIN seas. Temperature changes within this sea layer directly affected changes in steric height rises and stagnation in SSH rises.

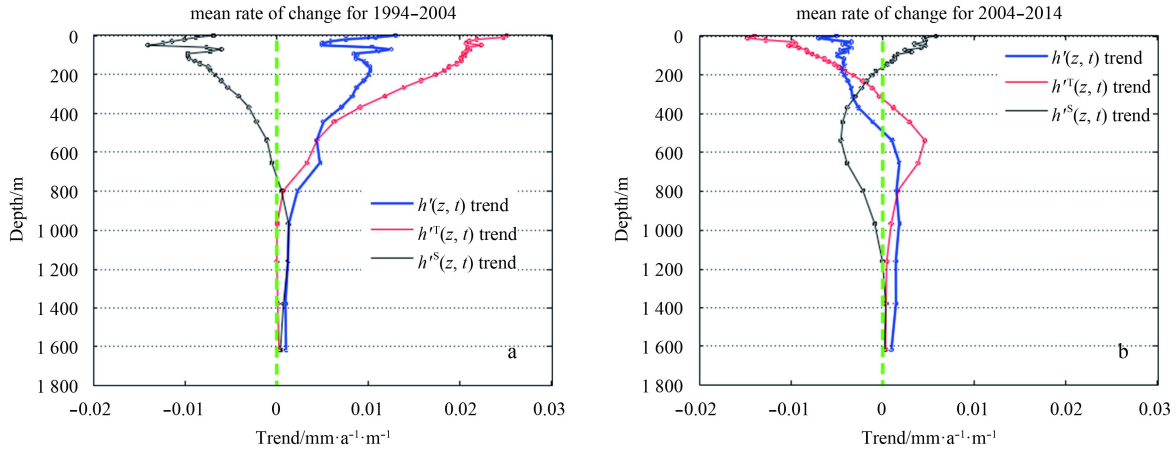

Fig. 6. Profiles of mean $h'(z, t)$, $h'^{T}(z, t)$, and $h'^{S}(z, t)$ trends for the Norwegian Sea basins.

4 Analyzing the mechanisms for stagnation of SSH rises

We have earlier explained that slowdown in SSH rises in the GIN seas during 1994–2014 was caused by stagnation of warming in the upper layer (0–600 m) of the Lofoten and Norwegian Basins. Air-sea flux and lateral or vertical fluxes within an ocean may cause denaturation of the upper water. Vertical exchanges within oceans are generally small. Figure 6 shows that water deeper than 600 m did not undergo any major change in property. Thus, the effect of vertical flux within the ocean on temperature changes of the upper water was minimal for these sea territories.

Although properties of the upper water of the GIN seas could have been affected by the rapid melting of the Greenland ice sheet (Marzeion et al., 2012), the latter process has regional variations, with only a small amount of melted ice entering the Greenland Sea. Furthermore, most of the meltwater in the GIN seas flows to the North Atlantic Ocean by the East Greenland Current, such that there is little impact on the internal portions of the GIN seas (Gardner et al., 2013; Straneo et al., 2012; Sutherl et al., 2014; Cox et al., 2010). Studies have shown that the upper water of the Norwegian Sea (shallower than 600 m) is affected by local air-sea flux, Atlantic inflow from the south, and Arctic water from the west (Rossby et al., 2009; Kushnir, 1994). Specifically, the Lofoten Basin is primarily affected by the Atlantic inflow, with its upper water mainly comprising Atlantic water (Köhl, 2007). In addition to the Atlantic warm water, the Norwegian Basin is also directly affected by cold freshwater from the Iceland Sea (Mork et al., 2014; Curry and Mauritzen, 2005). At the western portion of the GIN seas, cold water flows in from the Arctic Ocean by the East Greenland Current, during which it mixes continuously with the backflow of Atlantic water. The bulk of the water then flows south into the Northwest Atlantic Ocean, while only a small portion flows east to form the East Icelandic Current, (EIC), which then flows directly into the Norwegian Basin.

Some studies have pointed out that during certain periods, properties of the upper water of the Norwegian Sea are significantly affected by the cold Arctic water (Curry and Mauritzen, 2005). However, this occurs only during abnormal situations where strong North Winds accompany strong negative NAO (North Atlantic Oscillation) (Mork et al., 2014). Between 1993 and 2014, there was a moderate negative NAO only in 2010, but its internal wind field did not consist of anomalous strong North Winds (Fig. 2d in Mork et al., 2014). Thus, the EIC did not significantly affect the Norwegian Sea. Figure 5 shows that slowdown in the steric height rises in the Lofoten Basin was significantly greater than that for the Norwegian Basin region. This indicates that changes in the Atlantic inflow significantly affected the upper water of the Norwegian Sea. It can thus be comprehensively deducted that during this period, properties of the upper water of the Norwegian Sea was not affected much by the EIC. Instead, the Atlantic inflow had a more prominent influence.

Stagnation of SSH rises for the GIN seas in 1994–2014 was mainly the result of changes in steric height. Next, we focus on the Atlantic inflow and air-sea flux, and separately discuss the mechanisms behind the different trends of steric height during those two periods, so as to determine the main reason for stagnation of the SSH rises.

4.1 *Rapid rise in steric height: 1994–2004*

The mean steric height of the GIN seas rose rapidly during this period because of rapid warming and steady salinization of the upper water. We separately analyze the effects of the air-sea flux and Atlantic inflow.

4.1.1 *Effect of air-sea flux*

Total air-sea freshwater flux is obtained by subtracting evaporation from precipitation. Calculations show that total air-sea freshwater flux for the GIN seas did not present any significant change in trend over most of the sea territories. The linear rate of change for the remaining sea territories was generally within ±0.1 mm/(d·a) (Fig. 7b). The rate of change for SSH caused by the effect of salt was within ±1 mm/a (Appendix). Hence, evaporation and precipitation were not major factors behind the decline in the halosteric component of the GIN seas (salinization of the upper water).

Total air-sea heat flux is the summation of short- and longwave radiations, and latent and sensible heats. There was no significant linear trend for the total air-sea heat flux in the GIN seas during 1994–2004. However, there was a significant trend of oceanic thermal reduction only in the Greenland Sea, with a linear rate of approximately 5 W/(m^2·a), which could result in steric height rise by approximately 7 mm/a (Appendix). This would correspond to the rate of rise for the thermosteric component in that area (Fig. 5c).

There was no significant change in the trend of air-sea heat flux at the sea territories of the Lofoten Basin, even though rise of the thermosteric component was rapid. However, the rates of rise in sea surface temperature (SST) and surface air temperature (SAT) for the Norwegian Sea as obtained from ECMWF data were similar (Figs 8a–b). The mean rates of rise in SST and SAT for the Norwegian Sea were basically the same, at (13.0±2.8)×10^{-2} and (14.5±6.7)×10^{-2}°C/a, respectively. Since the density and specific heat capacity of air are far smaller than that of seawater, it would not be possible for atmospheric warming to drive the warming of the 0-600 m layer of the Norwegian Sea at a uniform rate (Fig. 9). It is more likely that rapid warming of the upper water of the Norwegian Sea was caused by the Atlantic inflow.

For the sea territories of the Norwegian Sea, EN4 and ECMWF data for rate of change of SST (Figs 8c and b, respectively) were consistent. There was also good conformity between the mean trends for both rates (Fig. 8d, correlation coefficient is 0.78). This shows that rapid warming of the upper water of the Norwegian Sea as determined using EN4 data was credible. However, SST trends derived from the two types of data were significantly different for the Greenland Sea. The ECMWF data showed a significant decline, whereas the EN4 data presented a slight increase. This discrepancy could be due to the different spatial resolutions of the two sets of data, as well as different data types: EN4 and ECMWF data were derived from the assimilation of sectional observational data and atmospheric forecast data, respectively.

Sectional observational data are not available for the Greenland Basin region (especially in winter), leading to greater uncertainty in the EN4 assimilation data (Siegismund et al., 2007; Good et al., 2013). In addition, rapid increases in the SST of the Norwegian Sea probably affected the assimilation results for this region, creating the false phenomenon of SST warming (Fig. 8c). The ECMWF data has a higher spatial resolution ((1/8)°) and better data quality (Dee et al., 2011; Uppala et al., 2005). As such, the decline in the SST of the Greenland Basin during this period should

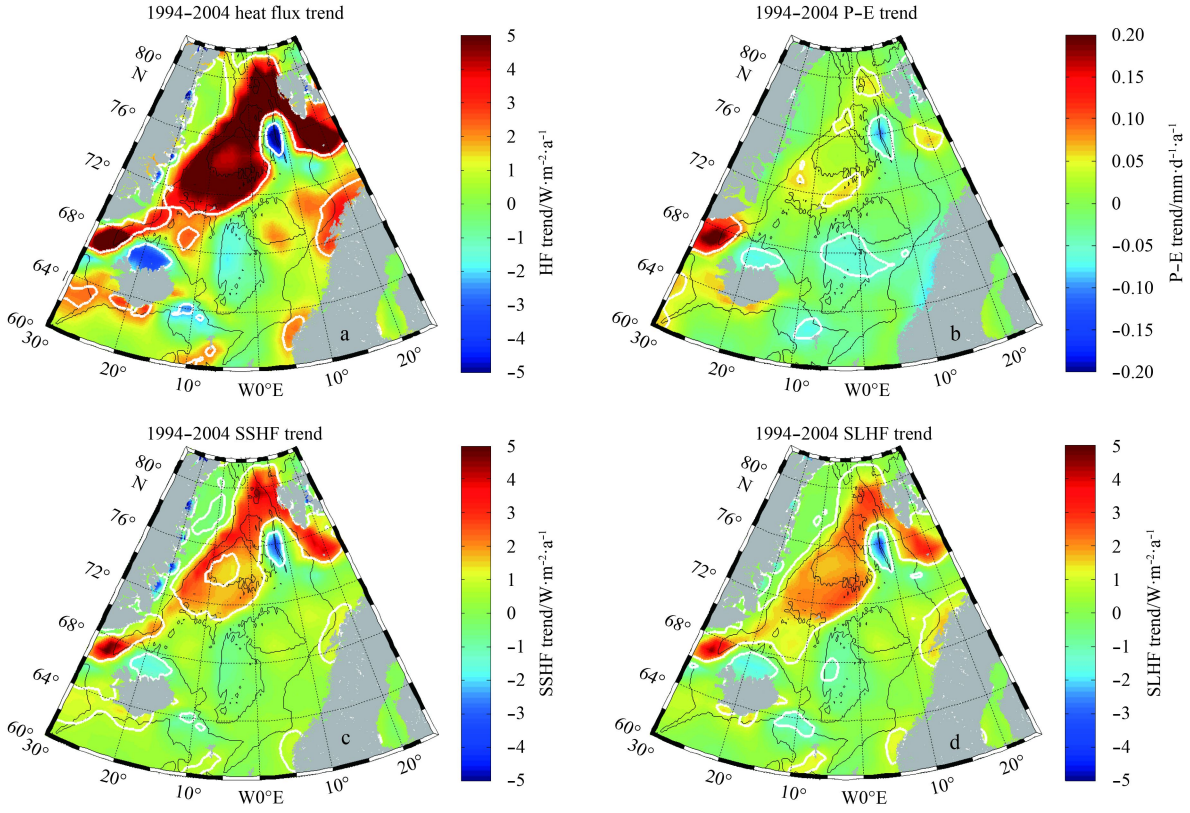

Fig. 7. Spatial distribution of linear trends of fluxes in 1994–2004. a. Total downward air-sea heat flux (HF), b. total downward air-sea freshwater flux (P-E), c. downward sensible heat flux (SSHF), and d. downward latent heat flux (SLHF).

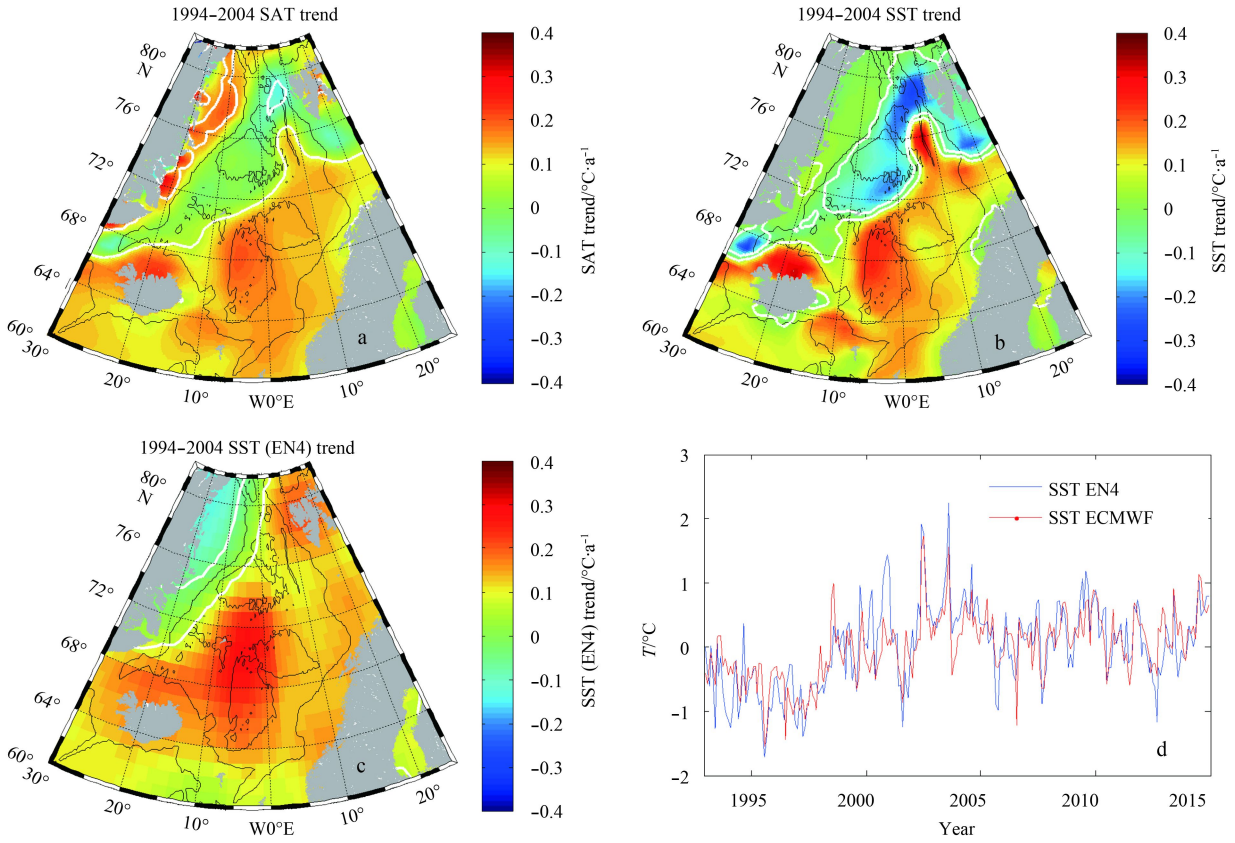

Fig. 8. Spatial distribution of SAT and SST trends during 1994–2004.

have greater credibility. This decline was not driven by the atmosphere because there was no significant reduction of the SAT during the period (Fig. 8a). Furthermore, there were increases in both downward latent and sensible heats (Figs 7c and d). Thus, the change must have been the result of oceanic processes.

The upper water of the Greenland Sea is covered by low-density (σ_θ<27.70) polar surface water (PSW) from the Fram Strait and melted sea ice (Rudels et al., 2002, 2005), which directly affect its SST. The SST obtained from ECMWF data exhibited opposite trends on both sides of the Mohn Ridge (Fig. 8b), thus eliminating the influence of Atlantic water. These results show that decline in the SST of the Greenland Sea was the result of low-density cold water from the Arctic Ocean covering or mixing with the upper water of the former. Considering the continuous backflow, mixing, and subsidence of warm water from the Atlantic Ocean with the mid-upper water of the Greenland Sea (250–800 m), the effect of the former should be more prominent (Perkin and Lewis, 1984; Rudels et al., 2002). In addition, there was a very obvious warming of Atlantic water within the Norwegian Sea during this period (Figs 8b and c), with the rate of warming far exceeding the rate of decline in the SST of the Greenland Sea SST. Therefore, it can be deduced that the mean temperature of the 1 500 m layer of the Greenland Sea should also increase. As such, although the surface of the Greenland Sea exhibited a cooling trend, it was still possible for mean temperature of the upper water to increase. This would be consistent with increases in the thermosteric component for these sea territories as calculated in this study (Fig. 5c). Overall, the decline in the SST of the Greenland Sea is a reasonable phenomenon that did not contradict the significant increase in the thermosteric component for the sea territories during the period as derived in this study.

4.1.2 *Atlantic inflow*

The Atlantic inflow, which has high temperature and salinity, can lead to denaturation of the upper water of the Norwegian Sea via two processes: changes in water properties or flow. Atlantic water with high salinity enters the GIN seas primarily through the channel between the Iceland-Faroe Islands and Shetland Islands. Sections of the water body shallower than 600 m and with salinity greater than 35.1 could be treated as Atlantic inflow water (AIW) (Wang et al., 2015). Figure 9a shows that the mean temperature of AIW had risen steadily in 1994–2004 at a rate of (5.3±1.9)×10^{-2}°C/a, while that for upper water of the Norwegian Sea basins (NUW) was even greater at (11.5±1.7)×10^{-2}°C/a. Increases in mean salinity for waters of the AIW and NUW were (2.9±2.1)×10^{-3} a^{-1} and (6.6±1.6)×10^{-3} a^{-1}, respectively.

The warming and salinization of the AIW was one of the reasons for the warming and salinization of the NUW. However, the AIW alone could not have sustained the rapid warming and salinization of the latter between 1994 and 2004. It was thus deduced that the trend for AIW during that period must have increased significantly as well, contributing to a large amount of the warming in NUW. Studies have also indicated that the warming of Atlantic inflow was synchronous with its increased flow (Mork et al., 2014; Furevik and Nilsen, 2005; Hátún et al., 2005.

Swift and Aagaard (1981) classified the upper water of the GIN seas into three main portions based on characteristics of the water mass. From east to west, these are the Norwegian warm water, transition zone water, and East Greenland cold water. Changes in the distribution of waters from the Atlantic and Arctic Oceans were analyzed on the basis of their respective characteristics. Specifically, the former, with high temperature and salinity, is carried by the Norwegian warm current, while the latter,

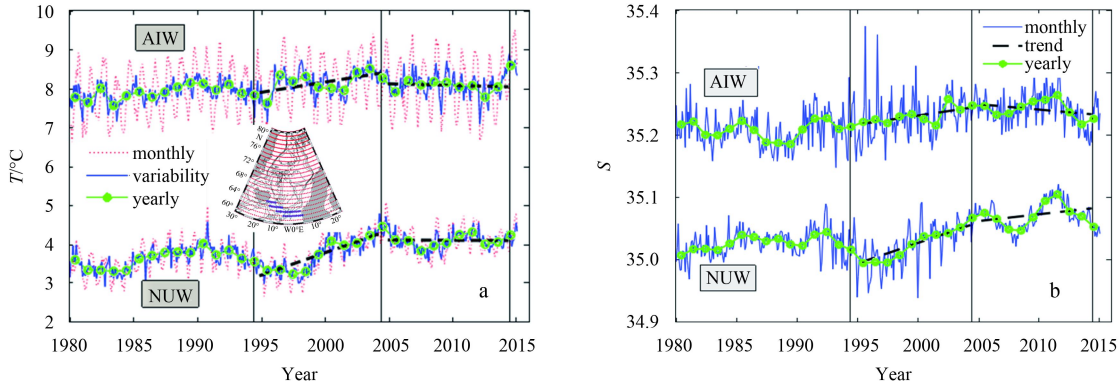

Fig. 9. Time series for Atlantic inflow and upper water of the Norwegian Sea. a. Mean temperature and b. salinity. In the positioning diagram, AIW (Atlantic inflow water) refers to water body shallower than 600 m (colored in blue) and with salinity greater than 35.1. NUW (upper water of the Norwegian Sea basins) refers to water body at 600 m layer of the shaded region in Fig. 3c. The broken lines in the diagram were obtained from segmented linear fitting of anomalous data.

with low temperature and salinity, is carried by the Greenland current. Water with T>2°C, S>35 water was selected as Norwegian Atlantic Water (NwAtW) (Hopkins, 1991), while that with T<0°C, S<34.4 was selected as Polar Water (PW) from the Arctic Ocean (Rudels et al., 2002, 2005).

The mean salinity of the NwAtW increased significantly ($(3.2\pm0.1)\times10^{-3}$ a^{-1}) (Fig. 10c) while the volume of PW did not change significantly (Fig. 10b). The contribution of air-sea freshwater flux to the salinity of the upper water was less than 1.0×10^{-3} a^{-1} (Appendix and Fig. 7b), with no significant change for most regions. After eliminating the effect of air-sea flux and polar water, it can be concluded that the increased salinity of the GIN seas was caused by the Atlantic inflow.

The increase in mean salinity of the NUW was at a similar rate with the increase in salinity of the AIW (Fig. 9b). However, the volume of the NwAtW had increased by 40% over that decade. In the absence of any other important factor, this could be due to substantial increases in its flow. Given the large differences in temperature between the NwAtW and transition zone water, the small amount of warming caused by the inflow (0.5°C) would not be responsible for the massive increase in volume of the NwAtW. Figures 8b, c and 4c show that during this period, the prominent region experiencing warming of the upper water was not along the main flow axis of the Norwegian warm current (at the eastern portion of the Norwegian Sea) but the Norwegian Sea basins region. This shows that after AIW entered the basin region with its increased flow, it significantly increased the temperature of the upper water. During this period, increases in the Atlantic inflow contributed significantly to the warming of the upper water of the GIN seas.

For the NwAtW, Fig. 10e shows that there was no significant rise in mean temperature during this period ($(1.7\pm2.0)\times10^{-2}$°C/a), and any rise was significantly less than that of the AIW (Fig. 9a). This shows that the increase in water volume of the NwAtW was not entirely from the inflow but rather, from the mixing of AIW and transition zone water. The latter has low temperature, which caused the decline in the temperature of the mixture. This was eventually reflected in the substantial increase in the volume of NwAtW without changing its mean temperature. Therefore, the increase in flow of the Norwegian current should be less than 40%.

Increased flow and salinity of the Atlantic inflow also resulted in significant salinization for most sea territories of the GIN seas, except for the shallow water at eastern Greenland (Fig. 5e). Since sea territories at eastern Greenland did not undergo significant salinization and the volume of PW did not decrease substantially, water input from the Arctic Ocean only increased slightly, preventing the warm water from entering the sea territories. This conclusion was further supported by the decline in mean temperature of PW during this period (Fig. 10f) and the absence of significant increase in salinity (Fig. 10d).

In short, the rapid increase in the steric height of the GIN seas during 1994–2004 was mainly caused by increased flow and thermohaline component of the Atlantic inflow, and the effect of air-sea flux was minor. These findings are consistent with the results of Skagseth and Mork (2012).

4.2 *Steady decline in steric height: 2004–2014*

4.2.1 *Air-sea flux*

There was no significant trend in the air-sea freshwater flux or heat flux over most of the territories of the GIN seas during this period. Thus, the air-sea flux component remained an unimportant factor (Fig. 11).

4.2.2 *Atlantic inflow*

Figure 9a shows that in 2004–2014, there was essentially no change in the mean temperature of the AIW and NUW (shallower than 600 m). However, the following events were observed: slight increase in the water volume of the NwAtW within the GIN seas ($(6.2\pm2.3)\times10^3$ km^3/a), significant decline in mean temperature ($-(3.9\pm1.6)\times10^{-2}$°C/a), and no change in mean salinity or total heat content of the water body (Fig. 10). It can be inferred that volume of the AIW did not increase significantly during this period, and that the slight increase in the volume was because the effect of mixing of waters from the NwAtW and transition zone was strengthened.

Given the large difference in temperature between NwAtW and transition zone and small difference in salinity, there was a significant decline in mean temperature of the NwAtW, with no change to its mean salinity. Being covered by NwAtW, the salinity of the upper water of the Lofoten Basin decreased significantly (increasing trend for SC, Fig. 5f). This is an indication of increased mixing. By eliminating the effects of the Atlantic inflow and air-sea flux, it could be inferred that the decline in input of Arctic freshwater was the main reason for the increase in mean salinity of the upper water of the GIN seas. During this period, there was a significant reduction in the volume of PW

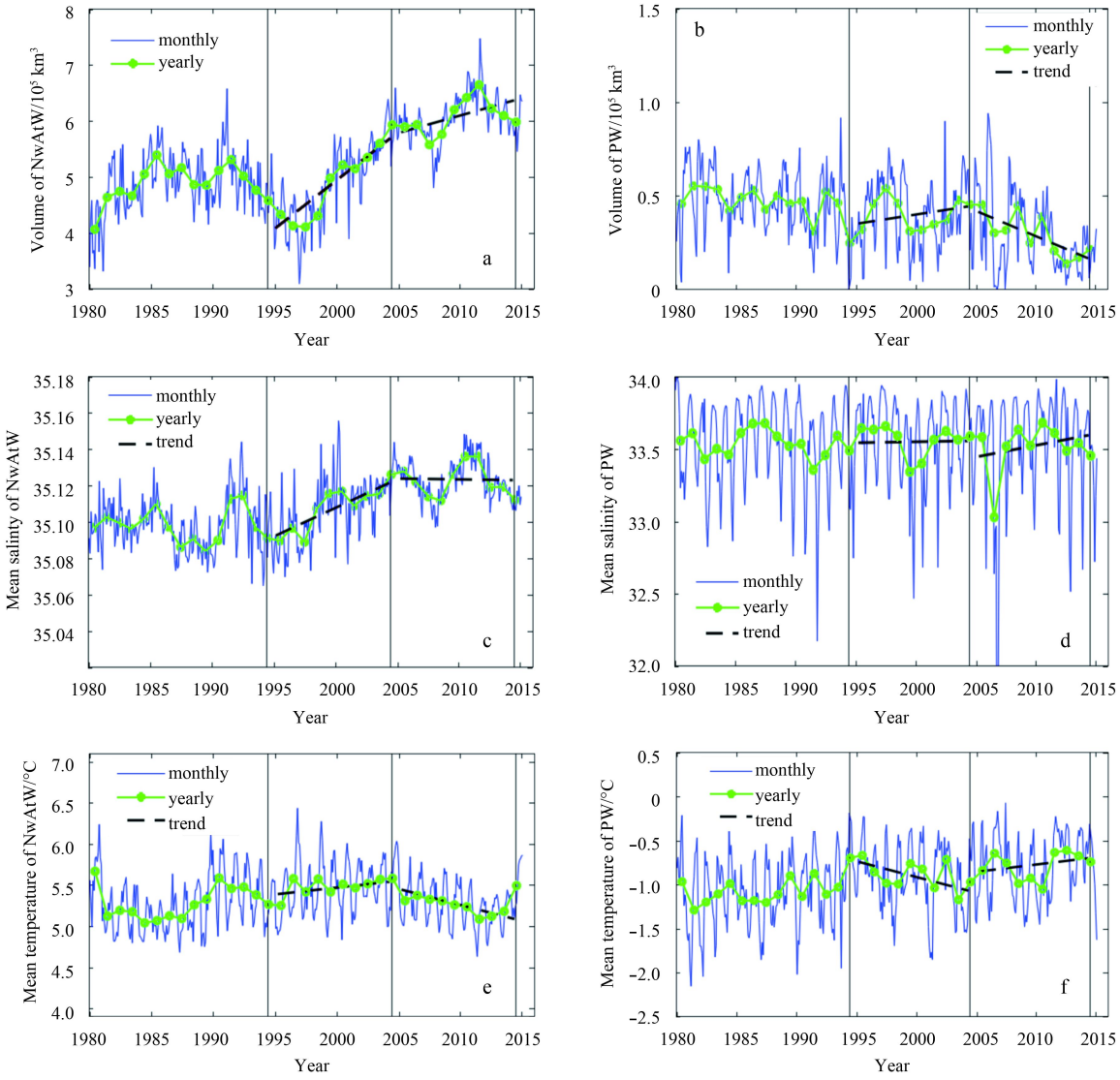

Fig. 10. Trends of water volume, mean temperature, and mean salinity. Respective trends within the GIN seas for the NwAtW (Norwegian Atlantic Water) (a, c and e) and for the PW (Polar Water) (b, d and f).

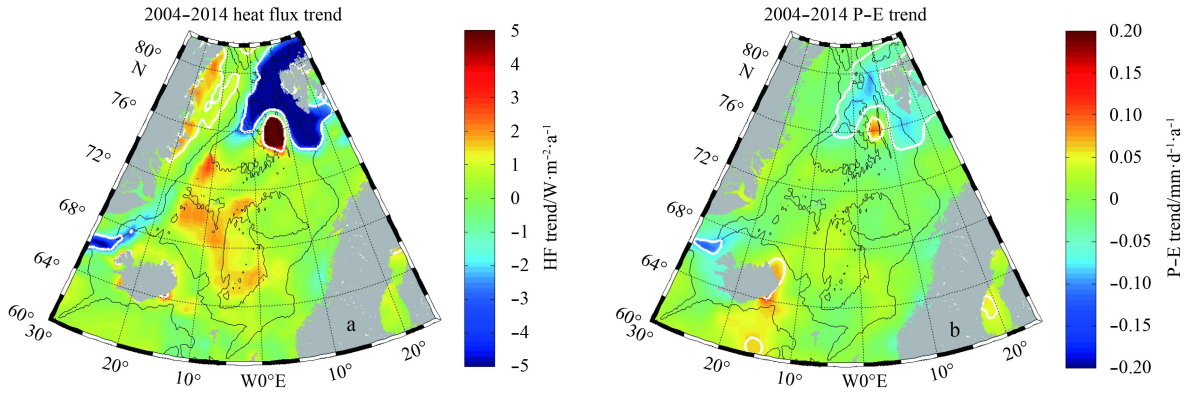

Fig. 11. Spatial distribution of trends for air-sea heat flux (a) and freshwater flux (b) during 2004–2014.

(–(2.7±1.2)×10^3 km^3/s) (Fig. 10b), with increased salinity in the East Greenland cold current (significant reduction in SC for this region, Fig. 5f), both of which support the aforementioned interpretation.

5 Conclusions

Around 2004, there was a notable slowdown of the mean SLA rise in the GIN seas. This phenomenon is very interesting and important, but has not been fully studied. Through comparative

analyses of linear rates of change for SLA and steric height during May 1994–April 2004 and May 2004–April 2014 combined with meteorological and hydrological data, the following conclusions were drawn:

(1) Mean SSH rises for the GIN seas during 1994–2004 and 2004–2014 were 4.4 and 1.4 mm/a, respectively. The magnitude of 3 mm/a far exceeded the global mean reduction (0.6 mm/a). In particular, steric height first increased and then decreased at an even greater magnitude of 4.5 mm/a. The rate of rise in the mass component also increased with a magnitude of 1.5 mm/a. The slowdown in the rise of the steric height of the GIN seas was mainly caused by the thermosteric component. The halosteric component declined steadily, with the rate maintained at 2 mm/a or more. Overall, the upper water of the GIN seas underwent steady salinization.

(2) Within the territories of the GIN seas, slowdown of SLA rises was especially prominent at the Norwegian Sea. Although its basin area accounts for only approximately 26% of the total area of the GIN seas, its contribution amounted to 50% of the total slowdown of the SLA rises. The slowdown of SSH rises in the Norwegian Sea was mainly caused by stagnation in warming of its upper water (shallower than 600 m).

(3) The temperature and salinity of the upper water of the GIN seas increased rapidly and gradually, respectively, as a result of the increased flow, significant warming, and slight increase in salinity of the Atlantic inflow in 1994–2004. This resulted in the rapid increase of its steric height. During 2004–2014, combined non-significant rise in flow and temperature of the Atlantic inflow caused stagnation in the warming of the upper water of the GIN seas. In contrast, the significant reduction in freshwater input from the Arctic Ocean led to a rise in the mean salinity of the upper water. Both factors contributed to the steady decline in the steric height of the GIN seas. Air-sea flux and Greenland's melting ice did not have much impact on the trends of steric height over the years. In summary, cessation in the increasing volume of the Atlantic inflow and warming of inflow water were the main factors responsible for the stagnation of SSH rises in the GIN seas.

Stagnation of SSH rises in the GIN seas has become a prominent phenomenon in recent years. Changes in the SSH of the GIN seas under the impact of global CC exhibited strong regional characteristics and were significantly influenced by the Atlantic inflow. Although NAO was weak during 1994–2004, thermal transportation from the Atlantic Ocean to the GIN seas increased significantly, causing rapid SSH rises. With global warming, the upper water of the Atlantic Ocean is likely to continue warming. If a strong NAO event were to occur simultaneously, the SSH of the GIN seas will rise even more rapidly. Thus, close attention should be paid to further developments in the SSH of the GIN seas and the feedback actions that these may have on the local (even global) circulation systems. However, there are still many research limitations and inadequacies. We only use AVISO data to get the slowdown rates of SSH rises in the Nordic seas, and simply use EN4 and ECMWF data to discuss the related mechanisms, data types in this paper are not quite enough to fully prove our conclusions and the errors of these data could greatly affect our result. So more observations and data are needed to study this phenomenon.

References

Ablain M, Cazenave A, Valladeau G, et al. 2009. A new assessment of the error budget of global mean sea level rate estimated by satellite altimetry over 1993–2008. Ocean Science, 5(2): 193–201

Antonov J I, Levitus S, Boyer T P. 2002. Steric sea level variations during 1957-1994: importance of salinity. Journal of Geophysical Research, 107(C12): SRF 14-1–SRF 14-8

Blindheim J, Østerhus S. 2005. The Nordic Seas, main oceanographic features. In: Drange H, Dokken T, Furevik T, et al., eds. The Nordic Seas: An Integrated Perspective. Washington: American Geophysical Union, 11–37

Carton J A, Chepurin G A, Reagan J, et al. 2011. Interannual to decadal variability of Atlantic Water in the Nordic and adjacent seas. Journal of Geophysical Research, 116(C11): doi: 10.1029/2011JC007102

Cazenave A, Dieng H B, Meyssignac B, et al. 2014. The rate of sea-level rise. Nature Climate Change, 4(5): 358–361

Cazenave A, Henry O, Munier S, et al. 2012. Estimating ENSO influence on the global mean sea level, 1993–2010. Marine Geodesy, 35(S1): 82–97

Chambers D P, Bonin J A. 2012. Evaluation of Release-05 GRACE time-variable gravity coefficients over the ocean. Ocean Science, 8(5): 859–868

Chen Xianyao, Tung K K. 2014. Varying planetary heat sink led to global-warming slowdown and acceleration. Science, 345(6199): 897–903

Cox K A, Stanford J D, Mcvicar A J, et al. 2010. Interannual variability of Arctic sea ice export into the East Greenland Current. Journal of Geophysical Research, 115(C12): C12063

Curry R, Mauritzen C. 2005. Dilution of the northern North Atlantic Ocean in recent decades. Science, 308(5729): 1772–1774

Dee D P, Uppala S M, Simmons A J, et al. 2011. The ERA-Interim reanalysis: configuration and performance of the data assimilation system. Quarterly Journal of the Royal Meteorological Society, 137(656): 553–597

Furevik T, Nilsen J E Ø. 2005. Large-scale atmospheric circulation variability and its impacts on the Nordic Seas ocean climate—A review. In: Drange H, Dokken T, Furevik T, et al., eds. The Nordic Seas: An Integrated Perspective. Washington: American Geophysical Union, 105–136

Gardner A S, Moholdt G, Cogley J G, et al. 2013. A reconciled estimate of glacier contributions to sea level rise: 2003 to 2009. Science, 340(6134): 852–857

Gill A E, Niller P P. 1973. The theory of the seasonal variability in the ocean. Deep Sea Research and Oceanographic Abstracts, 20(2): 141–177

Good S A, Martin M J, Rayner N A. 2013. EN4: quality controlled ocean temperature and salinity profiles and monthly objective analyses with uncertainty estimates. Journal of Geophysical Research, 118(12): 6704–6716

Hátún H, Sandø A B, Drange H, et al. 2005. Influence of the Atlantic subpolar gyre on the thermohaline circulation. Science, 309(5742): 1841–1844

Henry O, Prandi P, Llovel W, et al. 2012. Tide gauge-based sea level variations since 1950 along the Norwegian and Russian coasts of the Arctic Ocean: contribution of the steric and mass components. Journal of Geophysical Research, 117(C6): doi: 10.1029/2011JC007706

Hopkins T S. 1991. The GIN Sea—a synthesis of its physical oceanography and literature review 1972–1985. Earth-Science Reviews, 30(3–4): 175–318

IPCC. 2013. Climate Change 2013: The Physical Science Basis. Contribution of Working Group I to the Fifth Assessment Report of the Intergovernmental Panel on Climate Change. Cambridge, United Kingdom, New York, NY, USA: Cambridge University Press, 1535

Ivchenko V O, Danilov S D, Sidorenko D V, et al. 2007. Comparing the steric height in the Northern Atlantic with satellite altimetry. Ocean Science, 4(3): 441–457

Jiang Weiwei, Li Lei, Wang Chunhui, et al. 2011. A preliminary analysis on sea level change in the seas near the Greenland. Periodical of Ocean University of China (in Chinese), 41(10): 10–16

Köhl A. 2007. Generation and stability of a quasi-permanent vortex in the Lofoten Basin. Journal of Physical Oceanography, 37(11): 2637–2651

Kushnir Y. 1994. Interdecadal variations in north Atlantic sea surface temperature and associated atmospheric conditions. Journal of Climate, 7(1): 141–157

Marzeion B, Jarosch A H, Hofer M. 2012. Past and future sea-level change from the surface mass balance of glaciers. The Cryosphere, 6(6): 1295–1322

Mork K A, Skagseth Ø. 2005. Annual sea surface height variability in the Nordic Seas. In: Drange H, Dokken T, Furevik T, et al., eds. The Nordic Seas: An Integrated Perspective. Washington: American Geophysical Union, 51–64

Mork K A, Skagseth Ø, Ivshin V, et al. 2014. Advective and atmospheric forced changes in heat and fresh water content in the Norwegian Sea, 1951–2010. Geophysical Research Letters, 41(17): 6221–6228

Perkin R G, Lewis E L. 1984. Mixing in the west Spitsbergen current. Journal of Physical Oceanography, 14(8): 1315–1325

Rossby T, Prater M D, Søiland H. 2009. Pathways of inflow and dispersion of warm waters in the Nordic seas. Journal of Geophysical Research, 114(C4): C4011

Rudels B, Björk G, Nilsson J, et al. 2005. The interaction between waters from the Arctic Ocean and the Nordic Seas north of Fram Strait and along the East Greenland Current: results from the Arctic Ocean-02 Oden expedition. Journal of Marine Systems, 55(1–2): 1–30

Rudels B, Fahrbach E, Meincke J, et al. 2002. The East Greenland Current and its contribution to the Denmark Strait overflow. ICES Journal of Marine Science, 59(6): 1133–1154

Shao Qiuli, Zhao Jinping. 2015. Comparing the steric height in the Nordic Seas with satellite altimeter sea surface height. Acta Oceanologica Sinica, 34(7): 32–37

Siegismund F, Johannessen J, Drange H, et al. 2007. Steric height variability in the Nordic Seas. Journal of Geophysical Research, 112(C12): doi: 10.1029/2007JC004221

Skagseth Ø, Mork K A. 2012. Heat content in the Norwegian Sea, 1995–2010. ICES Journal of Marine Science, 69(5): 826–832

Straneo F, Sutherland D A, Holland D, et al. 2012. Characteristics of ocean waters reaching Greenland's glaciers. Annals of Glaciology, 53(60): 202–210

Sutherl D A, Roth G E, Hamilton G S, et al. 2014. Quantifying flow regimes in a Greenland glacial fjord using iceberg drifters. Geophysical Research Letters, 41(23): 8411–8420

Swift J H, Aagaard K. 1981. Seasonal transitions and water mass formation in the Iceland and Greenland seas. Deep Sea Research Part A. Oceanographic Research Papers, 28(10): 1107–1129

Tabata S, Thomas B, Ramsden D. 1986. Annual and interannual variability of steric sea level along line P in the northeast Pacific Ocean. Journal of Physical Oceanography, 16(8): 1378–1398

Tamisiea M E, Mitrovica J X. 2011. The moving boundaries of sea level change: understanding the origins of geographic variability. Oceanography, 24(2): 24–39

Uppala S M, Kållberg P W, Simmons A J, et al. 2005. The ERA-40 reanalysis. Quarterly Journal of the Royal Meteorological Society, 131(612): 2961–3012

Volkov D L, Landerer F W. 2013. Nonseasonal fluctuations of the Arctic Ocean mass observed by the GRACE satellites. Journal of Geophysical Research, 118(12): 6451–6460

Volkov D L, Pujol M I. 2012. Quality assessment of a satellite altimetry data product in the Nordic, Barents, and Kara seas. Journal of Geophysical Research, 117(C3): doi: 10.1029/2011JC007557

Wang Xiaoyu, Zhao Jinping, Li Tao, et al. 2015. Hydrographic features of the Norwegian Sea and the Greenland Sea in summer 2012. Advances in Earth Science (in Chinese), 30(3): 346–356

Appendix: Method for calculating changes in steric height caused by air-sea flux

Thermodynamic formulas can be used to determine temperature changes in the upper water column caused by air-sea heat flux, thereby deriving height changes of the water column. The specific formulas are as follows:

$$\Delta T \cdot H \cdot \rho \cdot C_p = \Delta E, \tag{A1}$$

$$\Delta h/H = \Delta T \cdot \alpha, \tag{A2}$$

where H represents height of the water column, ρ is mean density of water column, α is the thermal expansion coefficient, C_p is specific heat capacity of sea water, ΔE is change in heat flux, ΔT is the resultant change in temperature, and Δh is the resultant change to height of water column.

It was assumed that for water columns shallower than 600 m, changes in seawater properties caused by air-sea flux would be distributed uniformly (i.e., let H=600 m; this value does not affect the final result). Conditions of 35×10^{-3} and 10°C were adopted as typical properties for water in the Norwegian Sea (shallower than 600 m). When the specific heat capacity of sea water is 4×10^3 J/(kg·°C) and pressure P_z is approximately 3×10^6 Pa, the thermal expansion coefficient of seawater based on TEOS_10 is 1.715×10^{-4} K^{-1}. Simple calculations show that changes in heat flux amounting to 1.0 W/(m^2·a) can result in the following changes for the upper water (shallower than 600 m): rate of warming is 1.31×10^{-2}°C/a and rate of rise in steric height is approximately 1.4 mm/a.

The law of conservation of salinity can be used to obtain changes in salinity of the upper water arising from air-sea freshwater flux, thereby determining the resultant changes to the height of the water column. The specific formulas are as follows:

$$\Delta S \cdot H = S \cdot \Delta P, \tag{A3}$$

$$\Delta h/H = \Delta S \cdot \beta, \tag{A4}$$

where β is the saline contraction coefficient, ΔP is change in freshwater flux, and ΔS is the resultant change in salinity.

The calculation formulas for changes in SSH caused by freshwater flux are similar to that for heat flux (Eqs (A3) and (A4) above), adopting a β (saline contraction coefficient) of 7.538×10^{-4}. If the rate of change in air-sea freshwater flux is 0.1 mm/(d·a), the change in mean salinity for the upper water (shallower than 600 m) would be 2.1×10^{-3} a^{-1}, while the resultant rate of change in steric height would be 1.0 mm/a.